Steepest-entropy-ascent quantum thermodynamic modeling of decoherence in two different microscopic composite systems

Sergio Cano-Andrade,[1,*] Gian Paolo Beretta,[2,†] and Michael R. von Spakovsky[1,‡]
[1]*Department of Mechanical Engineering, Virginia Polytechnic Institute and State University, Blacksburg, Virginia 24061, USA*
[2]*Department of Mechanical and Industrial Engineering, Università di Brescia, Brescia 25123, Italy*
(Received 17 August 2014; published 30 January 2015)

The steepest-entropy-ascent quantum thermodynamic (SEAQT) framework is used to model the decoherence that occurs during the state evolution of two different microscopic composite systems. The test cases are a two-spin-$\frac{1}{2}$-particle composite system and a particle-photon field composite system like that experimentally studied in cavity quantum electrodynamics. The first system is used to study the characteristics of the nonlinear equation of motion of the SEAQT framework when modeling the state evolution of a microscopic composite system with particular interest in the phenomenon of decoherence. The second system is used to compare the numerical predictions of the SEAQT framework with experimental cavity quantum electrodynamic data available in the literature. For the two different numerical cases presented, the time evolution of the density operator of the composite system as well as that of the reduced operators belonging to the two constituents is traced from an initial nonequilibrium state of the composite along its relaxation towards stable equilibrium. Results show for both cases how the initial entanglement and coherence is dissipated during the state relaxation towards a state of stable equilibrium.

DOI: 10.1103/PhysRevA.91.013848 PACS number(s): 42.50.Pq, 03.65.Yz

I. INTRODUCTION

Much work has been devoted to the area of nonequilibrium dynamics with the general aim to develop a deeper understanding of the transition between microscopic and macroscopic physics [1,2] that could result in more effective control skills for the development of new technologies. This applies at all spatial and temporal scales of analysis. Of particular interest has been the consideration of the nonequilibrium phenomena that occur at the nanoscale, particularly in relation to quantum computing [3], quantum information [4,5], quantum cryptography [6], and quantum teleportation [7] where quantum entanglement, coherence, and decoherence are of importance.

A common approach to modeling these phenomena is to use linear Markovian quantum master equations (QMEs), i.e., those of the Kossakowski-Lindblad-Gorini-Sudarshan type [8–10], based on the so-called open-system model, which assumes that the system is attached to and weakly interacts with a thermal bath (reservoir or environment). As a result, quantum entanglement or coherence between system and reservoir cyclically builds up and then dissipates (i.e., the system and reservoir decohere) in a time frame for each cycle significantly shorter than that of the system's state relaxation to stable equilibrium (i.e., the so-called Born-Markov approximation [11,12]). In this regard, the dissipation phenomenon results from a loss of information, i.e., of correlations. As argued in [13], this theory of quantum open systems [10,14–17] can be seen as a special case of the theory of typicality [17–22] from which the laws of thermodynamics, the second law in particular, are said to emerge.

Linear Markovian QMEs fit the dissipative behavior of simple systems well, making them good candidates to model a variety of physical phenomena [23]. However, they fail, among other things, to provide a proper description of the time evolution of the state of the system for more general or strongly coupled microscopic systems [24,25] primarily because the Born-Markov approximation fails when the coupling becomes strong [8], thus negating the very mechanism assumed to be the cause of the irreversible relaxation to stable equilibrium.

An alternative approach is one that rationalizes the dissipation (or irreversibility) by assuming that it is not an emergent effect of coarse graining and decoherence approximations but instead a fundamental phenomenon [13]. This idea can be traced back to work of Prigogine and co-workers [26–29] and Park and co-workers and Hatsopoulos and co-workers [30–36] as well as a few more recent contributors with diverse motivations [37–41]. Their work attempts to build thermodynamics and irreversibility directly into the quantum dynamical level of description based on the assumption that entropy and irreversibility have a microscopic foundation. A by-product of these attempts has been the development of an explicit geometrically based mathematical formulation of a locally dissipative nonlinear gradient dynamics that can be used to model decoherence between strongly interacting subsystems of an overall isolated system. In this model, the time evolution of the overall density operator results from the interplay between the usual Hamiltonian dynamics driven by the interactions between subsystems and a phenomenological description of the dynamics of dissipation and decoherence whereby the reduced density operators of each subsystem are irreversibly attracted in the locally perceived direction of steepest entropy ascent (SEA) [42–44]. Though not conclusive, empirical comparisons presented in [45] and in the present paper suggest that the steepest-entropy-ascent construction in the quantum thermodynamic (SEAQT) framework may indeed provide a reasonable physical model for the phenomena of decoherence

*sergioca@vt.edu
†gianpaolo.beretta@unibs.it
‡vonspako@vt.edu

and decorrelation reported experimentally at a microscopic level [46–54].

Whereas the validity of the SEA construction as a phenomenological modeling tool is supported by its strong compatibility with the second law of thermodynamics as well as the differential geometric structure of most general theories of nonequilibrium [55], its potential implications at the fundamental level have remained controversial since its first introduction [56] and have recently been the subject of debates from several foundational points of view. The hypothesis that a fundamental nonlinearity may exist at the fundamental quantum level has often been criticized as incompatible with the so-called no-signaling condition. However, work by Ferreo *et al.* [57] suggests that, in principle, nonlinear quantum evolution is perfectly compatible with the impossibility of superluminal communication. Furthermore, the general criticism made in [58] against the existence of a fundamental nonlinearity, i.e., that nonlinear variants of Schrödinger's equation violate the second law of thermodynamics, is concerned with setting bounds not for possible modifications of the von Neumann equation for the time evolution of the density operator, but instead for possible modifications of the Schrödinger equation for the time evolution of the wave vector. Such modifications would deny that the evolution of pure quantum states is Hamiltonian. It is important, however, to note that for such states, the SEAQT equation of motion reduces to the Schrödinger equation, i.e., pure states remain pure states and evolve precisely according to Hamiltonian dynamics. From the point of view of thermodynamics, pure quantum states have zero (von Neumann) entropy since they are represented by idempotent density operators, i.e., projectors onto the linear span of a wave vector. Nonetheless, the presence of the additional nonlinear term in the SEAQT evolution equation makes such Hamiltonian, periodic evolutions of pure states mildly unstable limit cycles in the sense that mixed density operators in their vicinity slowly evolve away from the limit cycle [59] and, for a closed system, eventually arrive at a stable canonical state of maximum entropy, which is stable in the Lyapunov sense [60]. This stability is the strongest known form of compatibility with the second law of thermodynamics. In fact, Beretta [61] purposely designed the SEAQT equation of motion for the evolution of nonzero-entropy states (i.e., mixed density operators) around the need to encompass this stability requirement within the framework developed by Hatsopoulos and Gyftopoulos [31] as a test of the unorthodox ansatz that both the entropy and irreversibility might have microscopic foundations. The present paper does not address or take sides on any interpretational issue of this or any other sort. Rather, the focus is on the use of the SEAQT equation of motion in its version for composite systems [34] as a modeling tool, with the expressed objective of testing its potential usefulness in the phenomenological description of decoherence.

The description of dissipation by means of the locally perceived SEA construction effectively implements the principle of local maximum-entropy production (LMEP) and does so via the nonlinear SEAQT equation of motion [61], which consists of two terms. The first is the usual linear Hamiltonian term of standard unitary dynamics (Schrödinger–von Neumann equation) and the second is a structured nonlinear term designed to implement the LMEP principle subject to the relevant dynamical constraints [33,34,42,59,62]. Within the SEAQT framework, the idea is to treat the composite system as being isolated but in a mixed state, with the Hamiltonian describing as usual the internal interactions between subsystems and the nondissipative part of the time evolution, while the dissipative aspects of state evolution are left to the non-Hamiltonian term in the equation of motion. Of course, the physical explanation of such a phenomenological term is an interpretational issue that is beyond the stated scope of our paper. However, it is clear that among the possible interpretations, the most popular one is that dissipative effects are the results of unavoidable interactions between the microscopic system and its macroscopic surroundings, i.e., that the system is not truly isolated but interacts with some heat bath without a net exchange of energy between system and bath.

To illustrate the SEAQT approach, the phenomenon of decoherence for a microscopic system composed of two spin-$\frac{1}{2}$ particles is modeled as is a microscopic system composed of an atom-photon field such as that experimentally studied in cavity quantum electrodynamics (CQED) [47–49,63]. The paper is organized as follows. Section II describes the characteristics of the SEAQT framework. Section III presents some state functionals for the characterization of entanglement or coherence and correlation. Section IV provides a description of the model for the two-spin-$\frac{1}{2}$-particle microscopic composite system. Section V describes the CQED experiment by Brune *et al.* [63] and the model used here to numerically predict the experimental results. Section VI presents the SEAQT numerical results obtained for the two different models. Section VII presents a summary and draws some conclusions.

II. CHARACTERISTICS OF THE SEAQT EQUATION OF MOTION

The type of composite system of interest here to which the SEAQT equation of motion is applied [34] is an isolated and nonreactive composite system composed of M distinguishable constituents (i.e., each constituent may be a single particle, a group of indistinguishable constituents, or a field). The overall Hilbert space $\mathcal{H}$ is the outer product of the Hilbert spaces $\mathcal{H}^J$ of the individual constituents. The direct product of all individual spaces except the Jth one is denoted by $\mathcal{H}^{\bar{J}}$. Thus, the reduced density operator of the Jth constituent is $\rho_J = \mathrm{Tr}_{\bar{J}}\rho$, where ρ is the overall density operator. The identity operator may be written as $I = I_J \otimes I_{\bar{J}}$ and the overall Hamiltonian operator is denoted by H.

The time evolution of the overall density operator is assumed to obey an equation of motion in which the usual von Neumann term $-i[H,\rho]/\hbar$ competes with a dissipative term chosen so as to empirically model both irreversibility and decoherence, while satisfying a set of necessary conditions [64] for compatibility with thermodynamics and quantum nonlocality considerations. In particular, these conditions are: (i) separate energy conservation for two noninteracting subsystems (i.e., if $H = H_A \otimes I_B + I_A \otimes H_B$), (ii) the separate nondecrease of entropy (i.e., additivity of the entropy production rates) if two subsystems are in independent states (i.e., if $\rho = \rho_A \otimes \rho_B$), (iii) the independence of the local time evolutions of two subsystems if they are noninteracting and start in independent states, and (iv) the impossibility of locality problems such

as faster-than-light communication between noninteracting subsystems even if they are in entangled or correlated states; in particular, entanglement and correlations must not increase in the absence of interactions; this does not, however, mean that existing entanglement and/or correlations between A and B established by past interactions will have no influence on the time evolution of the local observables of either A or B.

The SEAQT dissipative term is designed to obtain a description of decoherence compatible with these conditions by assuming and implementing the principle of locally steepest entropy ascent whereby the effect of the dissipative term is to pull the density operator in a direction such that it is locally perceived by each subsystem as the direction of steepest entropy ascent (maximal entropy increase) as represented in state space, compatible with the symmetries and conservation constraints of the overall system. The strength of the pull in the locally perceived SEA direction is the only parameter of the model.

The implementation of the foregoing ideas requires precise definitions of what is meant by the locally perceived energy and entropy for a subsystem (in our case, the Jth constituent). Reference [34] proposes that such local observables should be represented by (mean field) local operators defined by

$$(H)^J \equiv \mathrm{Tr}_{\bar{J}}[(I_J \otimes \rho_{\bar{J}})H], \tag{1a}$$

$$(S)^J \equiv -k_B \mathrm{Tr}_{\bar{J}}[(I_J \otimes \rho_{\bar{J}})B \ln \rho]. \tag{1b}$$

Note that by virtue of the partial trace, $(H)^J$ and $(S)^J$ are operators on $\mathcal{H}^J$ that represent the partially averaged effect with respect to all other constituents for the given overall density operator. As such, from the local point of view of the Jth constituent, they represent the effective averaged local operators associated with the energy and the entropy. They are called the local effective perception of the overall Hamiltonian operator and of the overall entropy operator $-k_B\, B \ln \rho$, respectively. Their local mean values can be interpreted as the effective local perceptions, from the point of view of the Jth constituent, of the overall system's energy and entropy. A similar definition of local effective mean field operator has also been introduced in another quantum thermodynamics context (see, e.g., Eq. 4.11 of [65]). As pointed out in [43], it is noteworthy that when two subsystems are interacting, their local mean energies are (strictly speaking) hard to define because one does not know what fraction of the mean interaction energy should be attributed to one or the other. Similarly, when the states of the two subsystems are entangled or correlated, their local mean entropies are hard to define because one does not know what fraction of the correlation entropy should be attributed to one or the other. Nonetheless, the local mean values of the operators $(H)^J$ and $(S)^J$ given, respectively, by $\mathrm{Tr}[\rho_J (H)^J] = \mathrm{Tr}[(\rho_J \otimes \rho_{\bar{J}})H]$ and $\mathrm{Tr}[\rho_J (S)^J] = -k_B \mathrm{Tr}[(\rho_J \otimes \rho_{\bar{J}})B \ln \rho]$ are well-defined mean value state functionals, which represent each subsystem's local perception of the overall system's mean energy and entropy and coincide with the actual overall system's mean energy and entropy only if the subsystems are, respectively, noninteracting and uncorrelated.

In order to satisfy the nonlocality restriction expressed by condition (iv) above, the SEAQT model assumes a factorized expression for the dissipative term of the equation of motion, which takes the form

$$\frac{d\rho}{dt} = -\frac{i}{\hbar}[H,\rho] - \sum_{J=1}^{M} \frac{1}{\tau_J} D_J \otimes \rho_{\bar{J}}, \tag{2}$$

where the internal-relaxation times τ_J are considered to be positive constants or positive functionals of the density operator and each D_J is a traceless self-adjoint operator on $\mathcal{H}^J$ that is assumed (see below) to be a function of only ρ_J, $(H)^J$, and $(S)^J$. By partially tracing Eq. (2) over $\mathcal{H}^{\bar{J}}$, it is seen that each local density operator evolves according to the equation

$$\frac{d\rho_J}{dt} = -\frac{i}{\hbar}[H_J,\rho_J] - \frac{i}{\hbar}\mathrm{Tr}_{\bar{J}}[V_{J\,\bar{J}},\rho] - \frac{1}{\tau_J} D_J, \tag{3}$$

which shows that the global state ρ has a local effect not only through the interaction Hamiltonian $V_{J\bar{J}}$, which in general generates entanglement between interacting subsystems, but also through the dissipative term D_J via its dependence on ρ_J, $(H)^J$, and $(S)^J$, which must be defined in such a way that it destroys existing correlations without violating condition (iv). For example, when subsystem J is not interacting with subsystem $\bar{J}$, i.e., when $V_{J\bar{J}} = 0$, it should never be possible to influence the local observables of J by acting only on the Hamiltonian $H_{\bar{J}}$ of $\bar{J}$ (e.g., by switching on and off parameters or measurement devices within $\bar{J}$). That this property is indeed fulfilled by the form of the operators D_J proposed in [34] is still only conjecture, but is nonetheless confirmed heuristically via application. Of course, many other important features regarding thermodynamic compatibility, including conditions (i)–(iii) above, have been proven rigorously. For example, each local dissipative term separately conserves the overall system's mean energy and each subsystem's contribution to the overall system's rate of entropy production is positive semidefinite.

The key ansatz of the SEAQT model is that each dissipation operator D_J in Eq. (2) must be chosen so as to maximize the overall rate of entropy production subject to preserving the mean overall energy, the unit trace of the overall density operator, and an additional technical constraint. This constraint, as discussed in full detail in [44,62], is related to the geometrical fact that the SEA path in state space can only be identified with respect to a particular metric chosen to measure distances in state space, i.e., a proper measure of distance between density operators. Following the well-known arguments in [66–68], the SEAQT model selects the Fisher-Rao metric as the proper unique metric for the purpose of computing the distance between two probability distributions. With respect to this metric, Refs. [43,62] prove that the following explicit expressions of the dissipation operators D_J originally proposed in Ref. [34] indeed identify the SEA direction. These operators are nonlinear functions of the overall density operator and are defined as follows [34]:

$$D_J = \tfrac{1}{2}[\sqrt{\rho_J}\tilde{D}_J + (\sqrt{\rho_J}\tilde{D}_J)^\dagger], \tag{4}$$

with $\tilde{D}_J$ given by

$$\tilde{D}_J = \frac{\begin{vmatrix} \sqrt{\rho_J}(B\ln\rho)^J & \sqrt{\rho_J}(I)^J & \sqrt{\rho_J}(H)^J \\ (I,B\ln\rho)^J & (I,I)^J & (I,H)^J \\ (H,B\ln\rho)^J & (H,I)^J & (H,H)^J \end{vmatrix}}{\begin{vmatrix} (I,I)^J & (I,H)^J \\ (H,I)^J & (H,H)^J \end{vmatrix}}, \quad (5)$$

where B is the idempotent operator obtained by substituting unity for each nonzero eigenvalue of the density operator ρ (notice that B is essentially the projector onto the range of ρ so that the operator $B\ln\rho$ is always well defined, even when some of the eigenvalues of ρ are zero). Here $|.|$ denotes the determinant and $(F,G)^J$ for any operators F and G on $\mathcal{H}$ is expressed as

$$(F,G)^J = (\sqrt{\rho_J}(F)^J|\sqrt{\rho_J}(G)^J)^J, \quad (6)$$

where for any F_J and G_J on $\mathcal{H}^J$,

$$(F_J|G_J)^J = \tfrac{1}{2}\mathrm{Tr}_J(F_J^\dagger G_J + G_J^\dagger F_J). \quad (7)$$

Finally, the expectation value of the entropy for the overall, composite, microscopic system is given by the von Neumann entropy functional [69]

$$S = -k_B\,\mathrm{Tr}(\rho\ln\rho). \quad (8)$$

For the numerical simulations of the two-spin-$\frac{1}{2}$-particle system considered here, the internal-relaxation times τ_A and τ_B are assumed to be constants with a value of 1. For the atom-photon field simulations, they are based on characteristic times associated with the CQED experiments. Further details are given below.

The following general properties of Eq. (2) are proven in Ref. [34] and subsequent papers. The overall mean energy $E = \mathrm{Tr}(H\rho)$ is a constant of the motion. The entropy S is a nondecreasing function of time. The nondissipative density operators, i.e., those for which the dissipative term in Eq. (2) vanishes, are those and only those that satisfy for every J the condition that

$$\rho_J(B\ln\rho)^J = \rho_J[\lambda_{IJ}I_J + \lambda_{HJ}(H)^J], \quad (9)$$

where λ_{IJ} and λ_{HJ} are real scalars. If, in addition, ρ commutes with the Hamiltonian operator, then it represents an equilibrium state. Among the nondissipative states, the noteworthy density operators are those for the zero-entropy states and those for the maximum-entropy states. The zero-entropy density operators are in one-to-one correspondence with all the pure states of the standard quantum mechanical description for an isolated system. They evolve according to the standard Schrödinger–von Neumann unitary time evolution, exactly along the usual nondissipative trajectories. However, in the context of Eq. (2), these trajectories are the limit cycles of the complete dynamics of the dissipative system. The maximum-entropy density operators, i.e., the one-parameter family of canonical equilibrium states of thermodynamics where

$$\rho_{\mathrm{SE}}|_E = \frac{e^{-H/kT(E)}}{\mathrm{Tr}(e^{-H/kT(E)})} \quad (10)$$

and $\rho_{\mathrm{SE}}|_E$ maximizes $S = -k_B\,\mathrm{Tr}(\rho\ln\rho)$ for each given value of the overall mean energy $E = \mathrm{Tr}(H\rho)$, are the only equilibrium states of the dynamics described by Eq. (2) that are stable according to Lyapunov [60]. In other words, all other nondissipative equilibrium states are unstable. This last feature about the stability of the equilibrium states is a very strong form of thermodynamic consistency, which essentially implements and forces directly into the dynamical model the Hatsopoulos-Keenan statement of the second law of thermodynamics [70].

III. MEASURES OF ENTANGLEMENT OR CORRELATION AND DECOHERENCE

Since the scope of this paper is to model decoherence and decorrelation, measures for the entanglement of a pure state or the correlation of a mixed state as well as a measure for coherence must be adopted. For example, the following correlation functional was defined in [34] based on the subadditivity property of the von Neumann entropy functional:

$$\sigma_{AB}(\rho) = \mathrm{Tr}(\rho\ln\rho) - \mathrm{Tr}_A(\rho_A\ln\rho_A) - \mathrm{Tr}_B(\rho_B\ln\rho_B). \quad (11)$$

The rate of change of this correlation functional is expressed as

$$\frac{d[\sigma_{AB}(\rho)]}{dt} = \dot{\sigma}_{AB}|_H - \dot{\sigma}_{AB}|_D, \quad (12)$$

where the first term on the right-hand side represents the contribution of the Hamiltonian term on the right-hand side of Eq. (2), while the second term on the right-hand side of Eq. (12) represents the contribution of the dissipative term in Eq. (2). Based on the characteristics of Eq. (2), it is conjectured in [34] that the dissipative term can only destroy correlations between the subsystems so that $\dot{\sigma}_{AB}|_D$ should be non-negative at all times. A mathematical proof of the conjecture has not been worked out yet. However, our present numerical results seem to confirm its validity.

A measure of the coherence and correlation of the system is the trace norm of the commutator operator

$$\|C\| = \mathrm{Tr}(CC^\dagger), \quad (13)$$

where $C = i\,[H,\rho]$. The norm can be used as an indicator of how the off-diagonal elements of the matrix representing the state operator of the composite system evolve towards zero. Its time evolution can thus be thought of as a measure of the evolution of the loss of correlation among constituents. Equation (13) can also measure the time evolution of the loss of coherence of the constituents when applied to the reduced operators. Yet another measure of coherence and correlation, which provides a theoretical description of the experimental observations for a composite system formed by an atom and an electromagnetic field mode, such as those of CQED, is given by the two-atom correlation signal proposed in [48], i.e.,

$$\eta(t) = \tfrac{1}{2}e^{-2n(1-e^{-\gamma t})\sin^2\varphi}\cos[n(1-e^{-\gamma t})\sin 2\varphi], \quad (14)$$

where n is the average number of photons in the field mode, $\gamma = 1/T_R$, T_R is the photon lifetime in the cavity, t is the decoherence effective time, and φ is the field phase shift.

IV. TWO-SPIN-$\frac{1}{2}$-PARTICLE COMPOSITE SYSTEM

A. Energy eigenstructure of a two-spin-$\frac{1}{2}$-particle system

The first composite system considered here consists of two interacting spin-$\frac{1}{2}$-type particles. It is assumed that the local state of constituent A and that of B are fully represented in factor spaces $\mathcal{H}_A$ and $\mathcal{H}_B$, respectively. The Hilbert space corresponding to the composite system is given as the outer product of the two factor spaces such that

$$\mathcal{H} = \mathcal{H}_A \otimes \mathcal{H}_B. \tag{15}$$

When the particles interact, their states become correlated and the state or density operator ρ for the composite system may be written as

$$\rho = \rho_A \otimes \rho_B + \zeta. \tag{16}$$

In other words, by subtracting from ρ the outer product of the local state operators represented by the reduced state operators $\rho_A \equiv \mathrm{Tr}_B \rho$ and $\rho_B \equiv \mathrm{Tr}_A \rho$, a correlation operator ζ is obtained, which is the null operator only in the absence of correlations.

The Hamiltonian operator on $\mathcal{H}$, representing the total energy of the composite system and the generator of its standard quantum mechanical dynamics, is

$$H = H_A \otimes I_B + I_A \otimes H_B + V. \tag{17}$$

Here, for two identical spin-$\frac{1}{2}$-type particles A and B, it is assumed that

$$H_A = \tfrac{1}{2}\hbar\omega_0 \sigma_A^z, \tag{18a}$$

$$H_B = \tfrac{1}{2}\hbar\omega_0 \sigma_B^z, \tag{18b}$$

$$V = -\Gamma\, \vec{\sigma}_A \otimes \vec{\sigma}_B, \tag{18c}$$

where the $\vec{\sigma}_i$ ($i = A, B$) are three-dimensional vectors of Pauli operators, the σ_i^z are their z components, ω_0 is the transition frequency between the excited and ground energy levels of each particle, $\hbar$ is the reduced Planck constant, and Γ is the strength of the coupling between the subsystems. Thus, the assumed Hamiltonian is

$$H = -m\left(\sigma_A^z \otimes I_B + I_A \otimes \sigma_B^z\right) - \Gamma\,(\vec{\sigma}_A \otimes \vec{\sigma}_B), \tag{19}$$

where $m = \frac{1}{2}\hbar\omega_0$ is the unit strength of a uniform externally applied magnetic field in the z direction. The strength of the field given by $\vec{M} = m\hat{z}$ is small with respect to the Zeeman interaction splitting effects. For simplicity and without loss of generality, m and $\hbar$ are set to 1, while Γ is set to 0.02.

B. Construction of the initial entangled and correlated nonequilibrium state operators

Since one of the objectives here is to test numerically the condition that $\dot{\sigma}_{AB}|_D$, as determined by Eq. (2), is always non-negative, the initial density operators for the composite system are generated randomly according to the following procedure. To begin with, the one-to-one correspondence between the density operators ρ of a two-level system and points inside or on the Bloch sphere [3] is capitalized upon as is the fact that, for mixed states, the eigenprojectors of ρ are represented by opposite end points on the Bloch sphere of the diameter that passes through the point representing ρ. Therefore, the density operators of a two-level system belong to the three-parameter ($0 \leqslant \theta \leqslant \pi$, $0 \leqslant \phi \leqslant 2\pi$, and $0 \leqslant r \leqslant 1$) family

$$\rho = \tfrac{1}{2} I + \tfrac{1}{2} r\ \vec{P}(\theta,\phi) \cdot \vec{\sigma}, \tag{20}$$

where $\frac{1}{2}(1 \pm r)$ are the eigenvalues of ρ and the angles θ and ϕ denote the azimuth and zenith spherical coordinates, respectively, of the end point $\vec{P}(\theta,\phi)$ on the Bloch sphere of the ray that passes through the point representing ρ. The eigenprojectors of ρ are

$$P^{\pm}_{\theta,\phi} = \tfrac{1}{2} I \pm \tfrac{1}{2}\ \vec{P}(\theta,\phi) \cdot \vec{\sigma}. \tag{21}$$

Setting $r = 1$ and $\theta = 0,\pi$ in Eq. (20), the projectors $|0\rangle\langle 0|$ and $|1\rangle\langle 1|$, respectively, are obtained where $|0\rangle$ and $|1\rangle$ represent the orthonormal basis for which the Pauli operators are $\sigma^x = |0\rangle\langle 1| + |1\rangle\langle 0|$, $\sigma^y = -i\,|0\rangle\langle 1| + i\,|1\rangle\langle 0|$, and $\sigma^z = |0\rangle\langle 0| - |1\rangle\langle 1|$ and, of course, the identity operator is $I = |0\rangle\langle 0| + |1\rangle\langle 1|$. With respect to this basis, the eigenprojectors may be written more explicitly as

$$P^{+}_{\theta,\phi} = \cos^2\left(\frac{\theta}{2}\right)|0\rangle\langle 0| + \sin^2\left(\frac{\theta}{2}\right)|1\rangle\langle 1| + \sin\left(\frac{\theta}{2}\right) \times \cos\left(\frac{\theta}{2}\right)[\exp(-i\phi)\,|1\rangle\langle 0| + \exp(i\phi)\,|0\rangle\langle 1|\,], \tag{22}$$

$$P^{-}_{\theta,\phi} = P^{+}_{\theta+\pi,\phi+\pi}. \tag{23}$$

By randomly selecting the angles θ and ϕ, one spans between all possible orthogonal pairs $P^{+}_{\theta,\phi}$ and $P^{-}_{\theta,\phi}$ and hence all possible spectral resolutions of the identity operator $I = P^{+}_{\theta,\phi} + P^{-}_{\theta,\phi}$.

This construction for both subsystems A and B of our composite of two two-level systems is repeated, obtaining the two resolutions of the identity operators on the respective factor spaces $\mathcal{H}_A$ and $\mathcal{H}_B$,

$$I_A = P^{A+}_{\theta_A,\phi_A} + P^{A-}_{\theta_A,\phi_A}, \tag{24a}$$

$$I_B = P^{B+}_{\theta_B,\phi_B} + P^{B-}_{\theta_B,\phi_B}, \tag{24b}$$

and noticing that by randomly selecting the angles θ_A, ϕ_A, θ_B, and ϕ_B, ones spans between all possible spectral resolutions of the identity operator on the overall Hilbert space $\mathcal{H} = \mathcal{H}_A \otimes \mathcal{H}_B$,

$$I = P^{A+}_{\theta_A,\phi_A} \otimes P^{B+}_{\theta_B,\phi_B} + P^{A-}_{\theta_A,\phi_A} \otimes P^{B-}_{\theta_B,\phi_B} + P^{A+}_{\theta_A,\phi_A} \otimes P^{B-}_{\theta_B,\phi_B} + P^{A-}_{\theta_A,\phi_A} \otimes P^{B+}_{\theta_B,\phi_B}. \tag{25}$$

Therefore, the density operators of the composite of the two two-level systems belong to the family

$$\rho = \omega_{++} P^{A+}_{\theta_A,\phi_A} \otimes P^{B+}_{\theta_B,\phi_B} + \omega_{--} P^{A-}_{\theta_A,\phi_A} \otimes P^{B-}_{\theta_B,\phi_B} + \omega_{+-} P^{A+}_{\theta_A,\phi_A} \otimes P^{B-}_{\theta_B,\phi_B} + \omega_{-+} P^{A-}_{\theta_A,\phi_A} \otimes P^{B+}_{\theta_B,\phi_B}, \tag{26}$$

where the ω, being the eigenvalues of ρ, must be non-negative and sum to unity. The procedure to select random initial states is thus completed by generating four random number x_1, x_2, x_3, and x_4 between 0 and 1 and setting the ω based on

$$\omega_i = \frac{x_i}{\sum_i x_i} \tag{27}$$

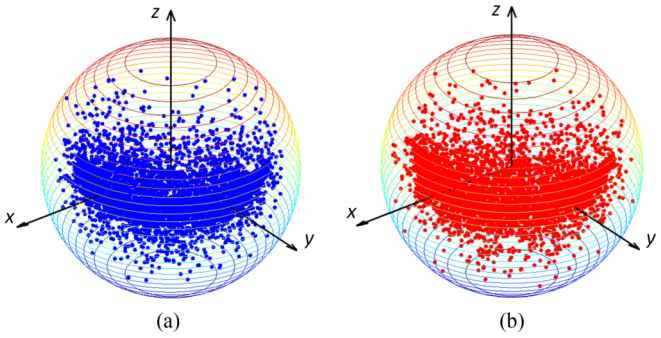

FIG. 1. (Color online) Bloch sphere representation of the reduced density operators $\rho_A \equiv \mathrm{Tr}_B \rho$ and $\rho_B \equiv \mathrm{Tr}_A \rho$ of the two subsystems corresponding to about 5000 randomly generated initial density operators ρ for the two-spin-$\frac{1}{2}$-particle composite system: (a) constituent A and (b) constituent B.

so that the conditions that they be non-negative and sum to unity are satisfied. To be more specific, for selecting randomly the angles $\theta_A, \phi_A, \theta_B$, and ϕ_B, the point picking approach given in [71] is used. In this scheme, four random numbers y_1, y_2, y_3, and y_4 between 0 and 1 are generated and then

$$\theta_A = \arccos(2y_2 - 1), \tag{28a}$$

$$\theta_B = \arccos(2y_4 - 1), \tag{28b}$$

$$\phi_A = \frac{2}{\pi} y_1, \tag{28c}$$

$$\phi_B = \frac{2}{\pi} y_3 \tag{28d}$$

are determined. Among the state operators that can be obtained with Eq. (26) is that for the final stable equilibrium state reached at the end of the state relaxation, which takes the canonical form given by Eq. (10) with the Hamiltonian operator given by Eq. (19). Figure 1 depicts the Bloch sphere representation of the reduced density operators for constituents A and B, corresponding to about 5000 randomly generated density operators. The time evolution of the energy eigenlevel occupation probabilities showing the energy redistribution within the energy eigenlevels of the system are found from

$$p_j = \langle P_{\varepsilon_j} \rangle = \mathrm{Tr}(P_{\varepsilon_j} \rho), \tag{29}$$

where the $P_{\varepsilon_j} = |\varepsilon_j\rangle\langle\varepsilon_j|$ are the eigenprojectors of the Hamiltonian operator.

V. PARTICLE-PHOTON FIELD COMPOSITE SYSTEM

A. Cavity quantum electrodynamic experiments and SEAQT modeling assumptions

The second composite system considered here consists of a particle-photon field such as those of CQED. The description of the experiments and the values used here in the modeling are based on the work developed by Haroche *et al.* [46–51,63].

A schematic representation of the experimental configuration is depicted in Fig. 2. Initially, Rb atoms are contained in an oven **B** from which one atom in eigenstate $|\psi_B\rangle = |0\rangle$ (excited level) is selected and subsequently subjected to a classical resonant microwave $\pi/2$ pulse in **R1** supplied by

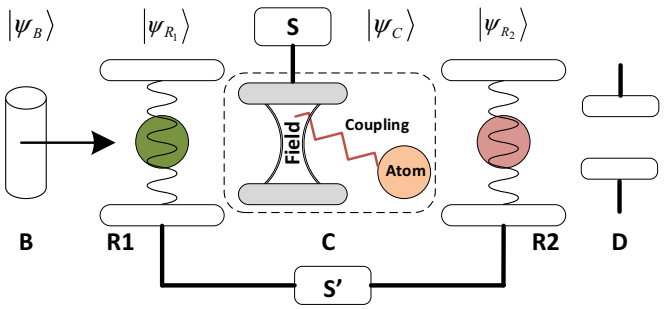

FIG. 2. (Color online) Schematic representation of an atom-field CQED experiment [47].

the source **S**′. This creates a state in a superposition of circular Rydberg eigenlevels $|0\rangle$ and $|1\rangle$ (ground level) for the atom, corresponding to principal quantum numbers 51 and 50, respectively. Afterward, the atom is allowed to enter the high-Q quantum cavity **C** that contains an electromagnetic field mode in a Fock state $|\alpha\rangle$ previously injected into the cavity by an external source **S**. The atom and cavity are off-resonance and therefore absorption of photons is not exhibited during the interaction. The atom only shifts the phase of the field mode by an amount φ. This phase shift causes the coupling of the excited level of the atom to the field mode state with phase $|\alpha_0\rangle \equiv |\alpha e^{i\varphi}\rangle$ and the coupling of the ground state of the atom to the field mode state with phase $|\alpha_1\rangle \equiv |\alpha e^{-i\varphi}\rangle$. In this manner, an entanglement between the states of the constituents is created such that

$$|\psi_C\rangle = \frac{1}{\sqrt{2}}(|0,\alpha_0\rangle + |1,\alpha_1\rangle). \tag{30}$$

After leaving the cavity, the atom is subjected again to a resonant microwave pulse in **R2** equal to that at **R1**, mixing the atom energy levels and creating a blurred state for the composite, which preserves the quantum ambiguity of the field phase such that

$$|\psi_{R_2}\rangle = \tfrac{1}{2} e^{-i\varphi} |0\rangle (|\alpha_0\rangle - |\alpha_1\rangle) + \tfrac{1}{2} |1\rangle (|\alpha_0\rangle + |\alpha_1\rangle). \tag{31}$$

Finally, the excited eigenlevel state of the Rb atom is observed and recorded by a detector **D**, projecting the state of the electromagnetic field into a superposition of coherent states $|\alpha_0\rangle$ and $|\alpha_1\rangle$. Since at this point the state of the atom has been unveiled, the only coherence left in the system is that belonging to the photon field.

In the SEAQT model, the detection of the first atom in $|0\rangle$ is simulated by assigning a value of 1 in Eq. (31) to the probability of finding the state of the atom in its excited level eigenstate so that, at this time, the coherence of the composite is due to the phase difference in the states of the field only. The initial thermodynamic state for the first atom-field composite system used in this model becomes

$$\rho_0 = |\psi_{R_2}\rangle\langle\psi_{R_2}|, \tag{32}$$

where the probability $P_e \approx 1$ of the atom being in its excited eigenlevel state is used. Equation (32) represents a pure (zero-entropy) state.

Since Eq. (2) evolves pure states into pure states, we need to slightly perturb the state ρ_0 given by Eq. (32) into a

neighboring mixed state. This activates the dissipative term in Eq. (2), which thereafter attracts the density operator towards thermodynamic equilibrium. The slight perturbation is obtained using the procedure suggested in [59], i.e., by assuming the initial state to be

$$\rho(0) = \lambda\rho_0 + (1-\lambda)\,\rho_{\rm SE}|_{E={\rm Tr}(H\rho_0)}, \tag{33}$$

where $\rho_{\rm SE}|_{E={\rm Tr}(H\rho_0)}$ is the stable equilibrium state given by Eq. (10). A value of $\lambda = 0.95$ is used in the perturbation in order to start the evolution from a nonequilibrium state very close to the original zero-entropy initial state ($\lambda = 1$) given by Eq. (32).

As the next step in the experiments, once the state of the photon field has been prepared in a Schrödinger cat state, the field is allowed to stay inside the cavity during a time t (decoherence time) in order to allow for decoherence, i.e., the loss of quantum superposition in the state of the field. In the SEAQT model, this relaxation is simulated by using Eq. (2) to drive the perturbed initial state operator of the first atom-field composite system given by Eq. (33) towards a state of thermodynamic equilibrium during a time t (decoherence time), which is equivalent to that of the experiments.

After the state of the first atom-field composite system has been allowed to relax (decohere) for a certain period of time t (again noting that this decoherence time is equivalent for both the experiments and the SEAQT model), the next step is to obtain an indicator of the coherence left in the field. In the experiments, to monitor the decoherence of the photon field without developing a direct measurement on it that causes the collapse of the quantum state, a second Rb atom with characteristics identical to those of the first one is put through the same path after the delay (or decoherence) time of t. This second atom also shifts the phase of the electromagnetic field, producing four phase components, of which two are zero because the second atom undoes the phase shift of the first atom and partially recombines the state components. If there is no decoherence (this would be possible only if $t = 0$), the probability of finding the second atom in the excited level eigenstate would be equal to one. On the other hand, if the photon field is allowed to relax (or decohere) for a certain period of time $t \neq 0$, the probability of finding the second atom in the excited level eigenstate would be lower than one. A certain number of events are recorded at each delay (or decoherence) time t and the average value is reported.

In the SEAQT model, numerical results of the evolution of the state of the first atom-field system are obtained at every instant of time, allowing one to observe the progressive decoherence of the field at every instant of time. Thus, the coherence of the field is tested by calculating the observable given by Eq. (13) from the numerical simulations. This is an indicator of how the off-diagonal elements in the density matrix of the first atom-field composite system decay with time. The decay of these off-diagonal elements is an indicator of the decoherence of the first atom-field composite system that is monitored experimentally in [63] and monitored using standard theory in [48] by taking advantage of the interference existent between the two atoms. As for the case of standard theory given by Eq. (14), the SEAQT decoherence indicator given by Eq. (13) provides a value of 0.5 if no decoherence has taken place and a value of 0 if the first atom-field composite system is in a fully incoherent statistical mixture.

For this first atom-field SEAQT model and consistent with standard theory (see the choice of the relaxation constant κ in [50]), the internal relaxation times τ_J are assumed to be a function of the residence time T_R of the field in the cavity, i.e., $\tau_J = \alpha T_R$, where α is a positive constant chosen so that τ_J is close to the characteristic decoherence time reported for the experiment (see Sec. VI and the discussion of Fig. 13). The nondimensional decoherence time is therefore given as it is for the case of the experiments and standard theory, as t/T_R.

B. Atom-field Jaynes-Cummings Hamiltonian

In the modeling of a composite field mode-atom system, it is usually assumed that the single mode of an electromagnetic field is quantized and treated as a two-level-type harmonic oscillator fully represented in a two-dimensional Hilbert space $\mathcal{H}_F$, while the atom is treated as a two-level-type spin-$\frac{1}{2}$ particle fully represented in space $\mathcal{H}_A$ [72–74]. The Hamiltonian on $\mathcal{H} = \mathcal{H}_A \otimes \mathcal{H}_F$ describing the total energy of the composite is the traditional Jaynes-Cummings Hamiltonian [75–77] (in the rotating-wave approximation) such that

$$H = \tfrac{1}{2}\hbar\omega_{eg}(\sigma^z \otimes I_F) + \hbar\omega_f(I_A \otimes N) + V, \tag{34}$$

where the first term on the right-hand side is the Hamiltonian of the noninteracting particle, the second term is the Hamiltonian of the noninteracting photon field mode, and V is the interaction operator given by

$$V = \tfrac{1}{2}\hbar\Omega_0(a \otimes \sigma_+ + a^\dagger \otimes \sigma_-), \tag{35}$$

where $\hbar$ is the reduced Planck constant, σ^z is the z Pauli operator, σ_+ and σ_- are the raising and lowering (spin-flip) operators, $a^\dagger$ and a are the creation and annihilation operators, $N = a^\dagger a$ is the photon number operator, ω_{eg} is the transition frequency between the excited and ground energy levels of the atom, ω_f is the cavity frequency, and Ω_0 is the Rabi frequency, which indicates the strength of the atom-field interaction.

For the present model, values taken from [63] are used. The transition frequency between the excited and ground energy levels of the atom is $\omega_{eg}/2\pi = 51.099\,{\rm GHz}$ and the Rabi frequency is $\Omega_0/2\pi = 24\,{\rm kHz}$. Detuning parameters of $\delta/2\pi = 70$ and $170\,{\rm kHz}$, corresponding to phase shifts of $2\varphi = 100^\circ$ and 50°, respectively, and where $\delta = \omega_{eg} - \omega_f$ are also used.

VI. NUMERICAL RESULTS

A. Two-spin-$\frac{1}{2}$-particle composite system

Figure 3 shows an energy-entropy ($\langle E\rangle - \langle S\rangle$) diagram for the state evolution of the system. The four points depicted inside the curve are possible initial nonequilibrium states obtained with the approach described in Sec. IV B and illustrate the fact that any nonequilibrium state can be modeled with the approach used in this paper. Although state A_1 and states B_1, B_2, B_3, and B_4 are all modeled in terms of their evolution towards a state of stable equilibrium, the focus here is on the evolution of state A_1 only, for which a complete set of results is presented. With this in mind, the system evolves at constant

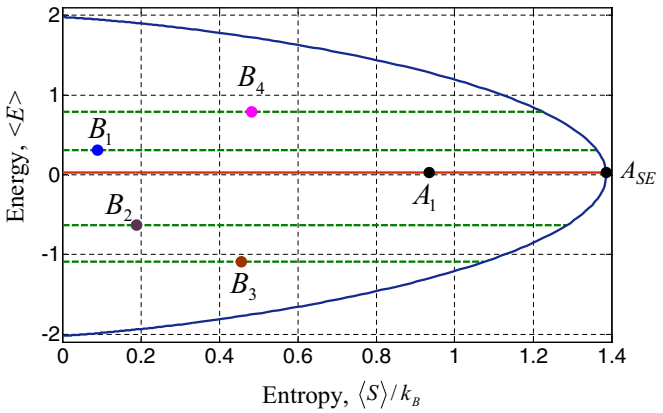

FIG. 3. (Color online) Energy-entropy diagram for the state evolution of the two-spin-$\frac{1}{2}$-particle composite system. States A_1 and A_{SE} are for the particular case presented in detail in the following figures, while states B_i are other possible initial nonequilibrium states generated.

energy from state A_1 towards the state of stable equilibrium at A_{SE} that for this case just happens to have a high negative absolute temperature. When the state of the system reaches A_{SE}, the density operator takes the canonical form of Eq. (10).

Figure 4 shows the norm of the commutator operator defined by Eq. (13). The evolution of the norm is taken as an indicator of how the off-diagonal elements of the matrix represent the density operator decay; as a result, it is also an indicator of how the coherence of the system disappears as the state of the system evolves towards A_{SE}. A drastic descent is observed at the beginning of the evolution because the coherence of the system is being annihilated by the dissipative term of the SEAQT equation of motion. This drastic descent is in accord with the locally perceived SEA ansatz upon which the dynamical model is constructed. As seen in Fig. 5(a) where the evolution of the composite system entropy is given, the entropy increases very rapidly at the beginning of the evolution and then quickly slows its increase, asymptotically approaching its stable equilibrium value. Figure 5(b) depicts the entropy

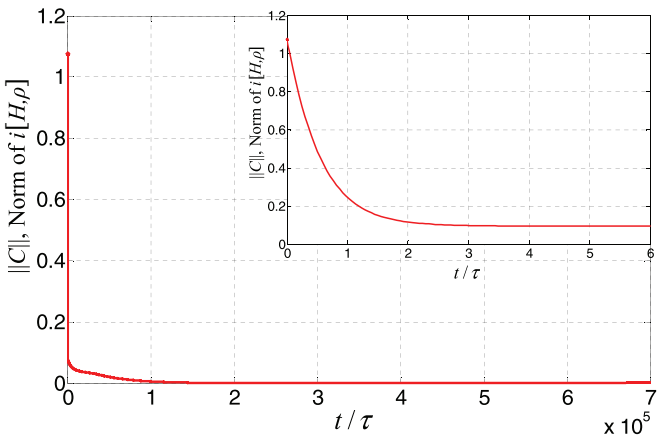

FIG. 4. (Color online) Evolution of $||C||$, which is the norm of the commutator term $C = i[H, \rho]$ for the two-particle composite system.

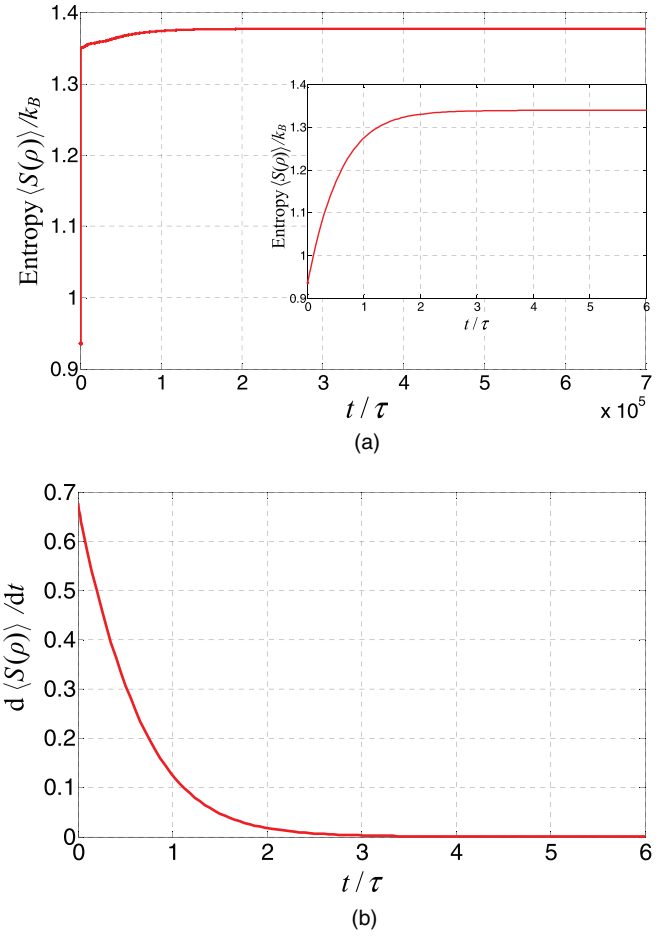

FIG. 5. (Color online) (a) Entropy and (b) entropy generation rate evolution for the two-spin-$\frac{1}{2}$-particle composite system.

generation rate evolution of the composite system where it can be observed that $d\langle S\rangle/dt$ remains non-negative at all times.

Figure 6 shows the x, y, and z components of the vector state representation for both constituents. It can be seen that constituent A starts its evolution closer to the surface of its corresponding unit sphere than constituent B. The red line corresponds to the z component of the vector state, which shows how the two constituents are coherently exchanging energy, i.e., when the energy of constituent A decreases, that of constituent B increases. The x and y components evolve very fast towards a value of zero, which is reached at a dimensionless time of about 10. This evolution towards the center of the local Bloch sphere represents the loss of local coherence of the constituents. In contrast, the nonlocal coherence belonging to the off-diagonal elements of the density matrix of the system continues its decay but at a very gradual rate until it reaches a value of zero at which point the Hamiltonian and density operators commute and the state of the composite system is that of stable equilibrium (see Fig. 4 above). During this slow nonlinear and nonlocal decay, the constituents continue exchanging energy with each other.

Figure 7 shows the evolution in time of the energy eigenlevel occupation probabilities given by Eq. (29). As can be seen, the largest redistribution of system energy takes place primarily between two of the four energy eigenlevels

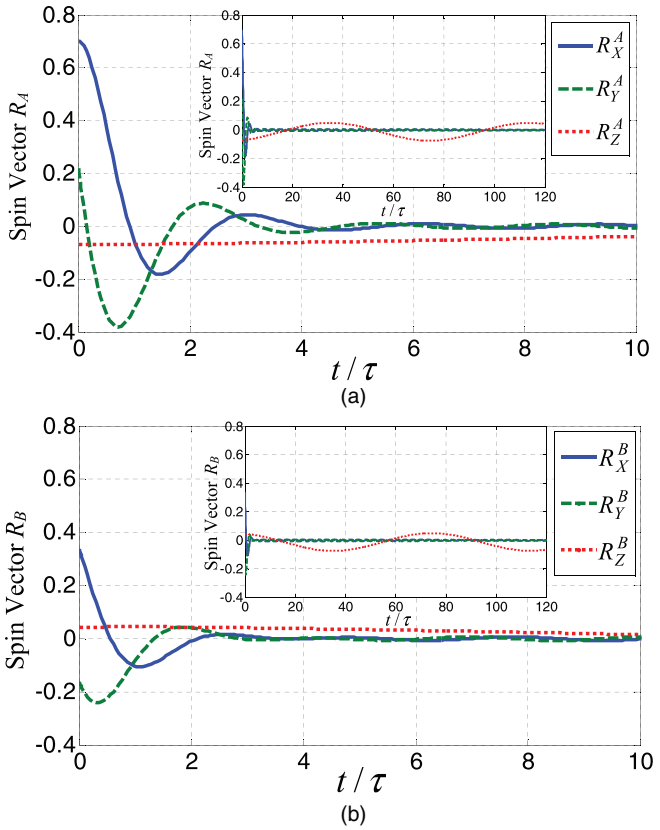

FIG. 6. (Color online) Evolution of the components of the state vector in their local Hilbert spaces: (a) constituent A (spin subsystem A) and (b) constituent B (spin subsystem B).

of the system, the majority of which occurs during a short nondimensional time interval corresponding to the decay of the local coherence of the constituents. After this fast initial redistribution, the redistribution of energy represented by changes in the eigenlevel occupation probabilities occurs at a much slower rate.

Figure 8 depicts the evolution in time of the entropy correlation functional defined in Eq. (11), which is a measurement of how the correlations between the constituents disappear

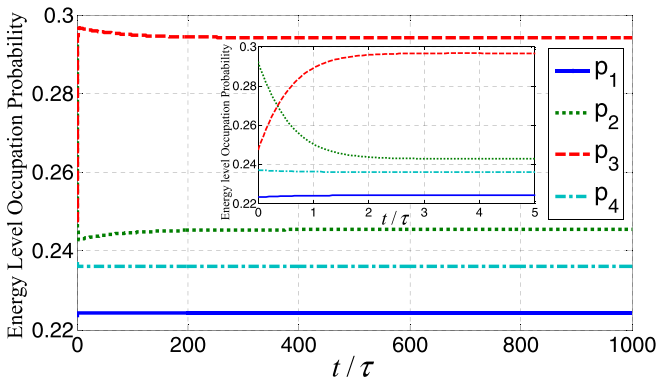

FIG. 7. (Color online) Evolution of the energy eigenlevel occupation probabilities of the composite system for a period of $t/\tau = 0$–1000.

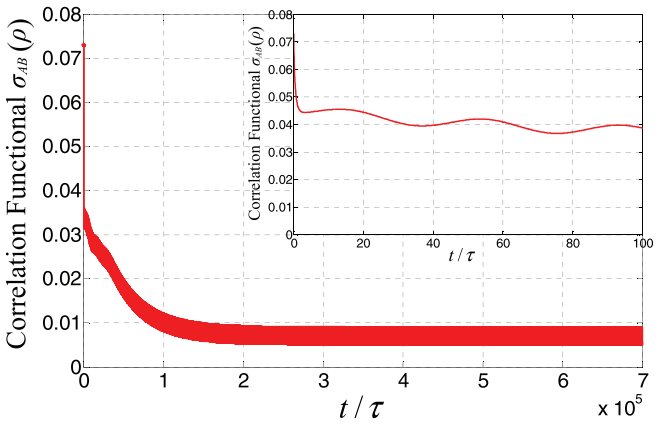

FIG. 8. (Color online) Evolution of the entropy correlation functional.

when the composite system evolves towards a state of stable equilibrium. The correlation functional reaches a constant value when the composite is at stable equilibrium, which occurs at about 7×10^5 dimensionless time units and at which the value of the correlation functional is $\sigma_{AB} = 0.0051$. The fact that the correlation functional does not reach a value of zero at stable equilibrium is because the interaction term V of the Hamiltonian operator of Eq. (18c) is continuously creating correlations. This creation of correlations is described by the contribution of the Hamiltonian term of the equation of motion to the rate of change of the correlation functional depicted in Fig. 9(a), where it can be observed that this rate of change oscillates continuously at a fixed amplitude even when the composite system is at stable equilibrium.

Figure 9(b) shows the rate of change of the correlation functional due to the dissipation term of the equation of motion and is consistent with the conjecture that the dissipation term can only destroy but never create correlations between constituents. Indeed, the rate of change of the entropy correlation is always non-negative. In an attempt to provide a broader study of this conjecture, 5000 different initial nonzero-entropy states are randomly generated as described in Sec. IV B. Figure 10 shows the degree of purity ($\bar{\gamma}_p = \mathrm{Tr}\rho^2$) of the density operator for the composite system for the 5000 different cases tested. In the figure, a value of $\bar{\gamma}_p = 1$ defines a state that is a pure state (i.e., one of zero entropy) and a value of $\bar{\gamma}_p = 0$ defines a state that is a stable equilibrium state for which the entropy is a maximum. The points in between represent nonzero-entropy nonequilibrium states with varying degrees of purity. It is observed that for this particular case, the majority of the state operators are located near a zone of purity of approximately 0.5. The closest state operator to stable equilibrium corresponds to one with a degree of purity of 0.28 and the state operator closest to the zero-entropy surface corresponds to one with a degree of purity of 0.86.

Figure 11 shows the rate of change of the contribution of the dissipative term to the rate of change of the entropy correlation functional $\dot{\sigma}_{AB}|_D$ for the different 5000 random initial nonequilibrium states tested. It can be observed that $\dot{\sigma}_{AB}|_D$ evolves to zero for all cases and remains non-negative at all times. The evolution of the initial nonequilibrium

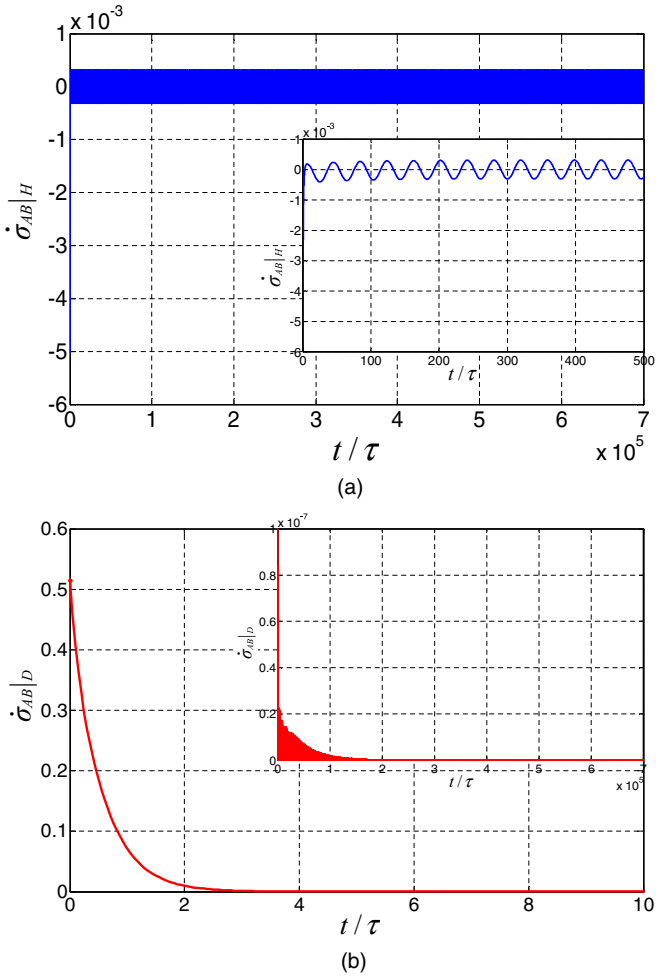

FIG. 9. (Color online) Rate of change of the contribution of the (a) Hamiltonian and (b) dissipative terms to the rate of change of the entropy correlation functional.

state located closer to stable equilibrium shows the lowest correlation so that the destruction of correlations is very low, i.e., close to zero. The evolution of the initial nonequilibrium state closest to a pure state shows an increase in the destruction of correlations at the beginning of the evolution, reaching a maximum at about $t/\tau = 0.6$ and then decreasing to zero. This increase in the rate of destruction of correlations early

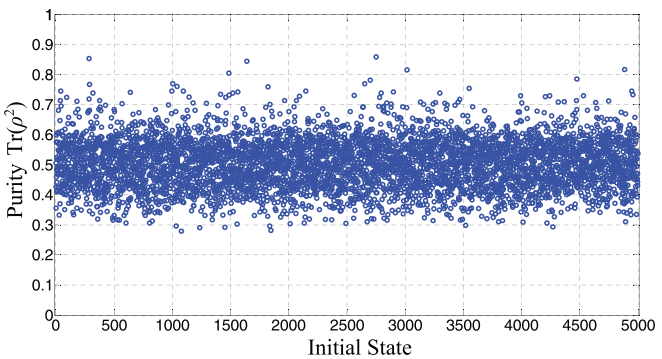

FIG. 10. (Color online) Degree of purity for the different 5000 random initial nonequilibrium states tested (same as in Fig. 1).

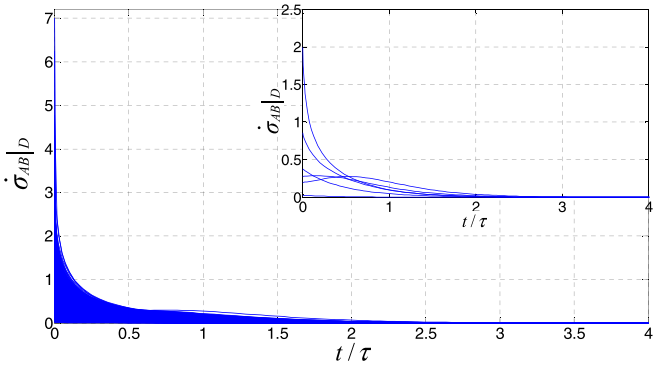

FIG. 11. (Color online) Rate of change of the contribution of the dissipative term to the rate of change of the entropy correlation functional for the different 5000 random initial nonequilibrium states tested. In the inset the evolution of six particular initial nonequilibrium states (i.e., with degrees of purity of 0.59, 0.58, 0.43, 0.68, 0.86, and 0.28) is depicted in order to show a more detailed evolution of $\dot{\sigma}_{AB}|_D$.

during the evolution also corresponds to an increase in the entropy production of the composite system. In other words, the entropy generation of the composite system increases as well for the first part of the evolution and then decreases, evolving towards zero.

Additional possible measures of decoherence are given by

$$K^H = \tfrac{1}{2}[\langle (H)^A\rangle + \langle (H)^B\rangle] - \langle H\rangle, \tag{36a}$$

$$K^S = \tfrac{1}{2}[\langle (S)^A\rangle + \langle (S)^B\rangle] - \langle S\rangle, \tag{36b}$$

which represent the difference in the locally perceived energies and the energy of the composite system and the difference in the locally perceived entropies and the entropy of the composite system, respectively. Figures 12(a) and 12(b) show the evolution of K^H and K^S, respectively, where it can be observed that these differences decay very quickly at first and then very gradually approach zero but never quite get there even at stable equilibrium, which occurs at about 7×10^5 dimensionless time units (not depicted in the figures).

B. Atom-photon field composite system

As was the case for the two-particle spin-$\frac{1}{2}$ system model, the evolution of the norm of the commutator operator given by Eq. (13) formed by the Hamiltonian and density operator for the atom-field mode composite system is used here to measure how the off-diagonal elements in the overall density or state matrix decay with time as the composite system evolves towards a state of stable equilibrium. When the atom is detected by the experiment in its excited level state, the state of the photon field is projected into a superposition of coherent states $|\alpha_0\rangle$ and $|\alpha_1\rangle$. Thus, the only coherence existing initially in the composite system is that belonging to the photon field. This coherence of the photon field is a maximum at the beginning of the state evolution. Consequently, the observable of the composite system captured by Eq. (13) is an indicator of how the coherence in the photon field is being dissipated in time.

In Fig. 13 the results of the SEAQT model are compared to the experimental data of [63] as well as to the theoretical

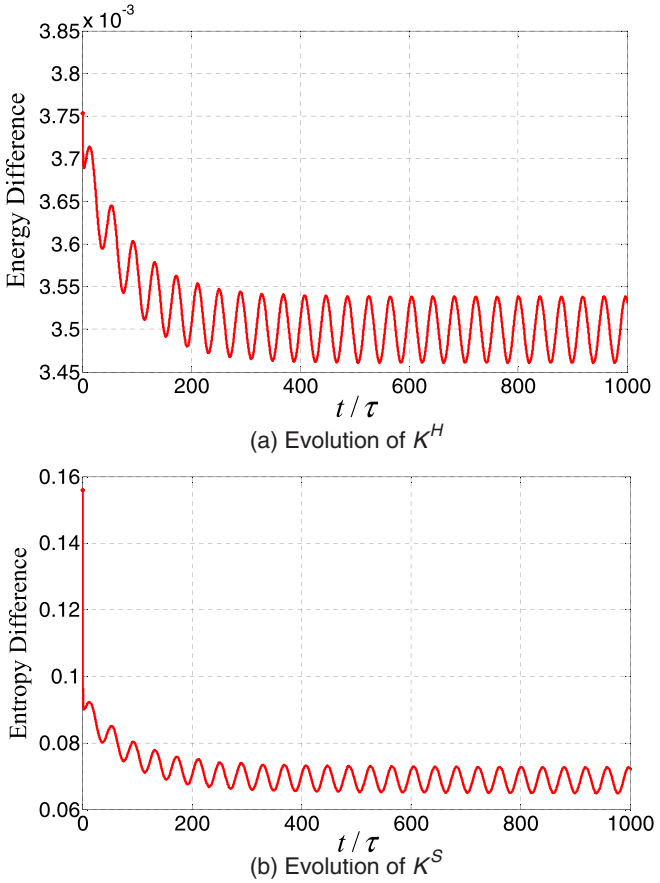

FIG. 12. (Color online) Evolution of the difference between the locally perceived energies and entropies of the constituents with respect to the energy and entropy of the composite: (a) K^H and (b) K^S.

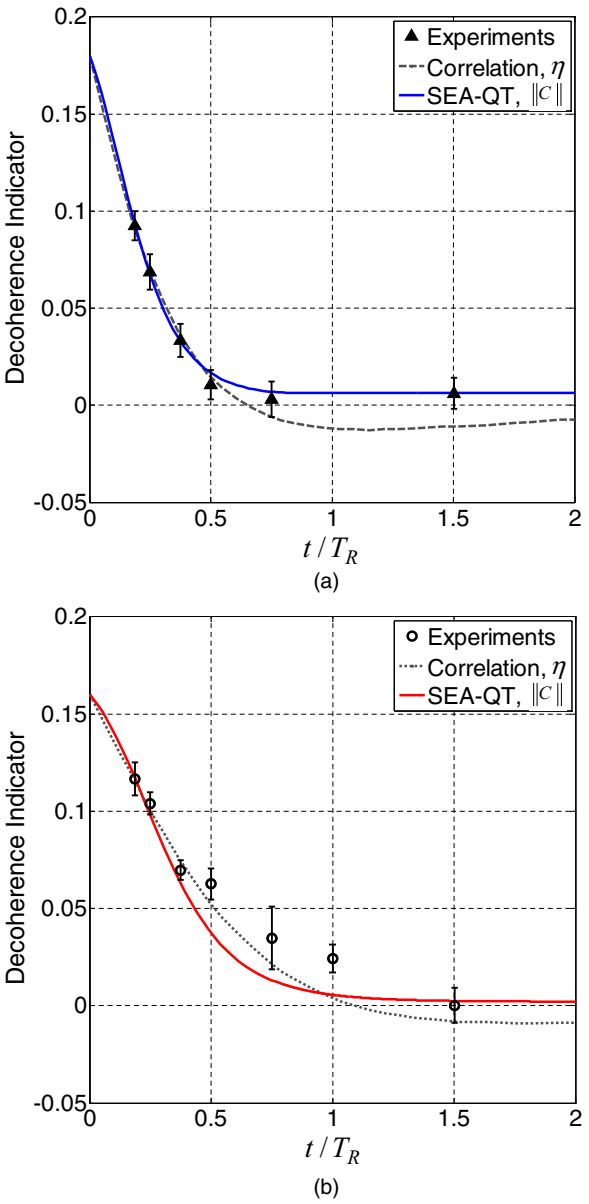

FIG. 13. (Color online) Comparison of the loss of coherence predicted by the SEAQT model with the CQED experimental results of [63] and theoretically calculated two-atom correlation signal $\eta(t)$ from [48] for two different values of the detuning: (a) detuning parameter $\delta/2\pi = 70$ kHz and (b) detuning parameter $\delta/2\pi = 170$ kHz.

prediction of the two-atom correlation signal $\eta(t)$ reported in the literature by Raimond *et al.* [48] and given by Eq. (14). Figure 13(a) depicts the comparison for a case with the detuning parameter $\delta/2\pi = 70$ kHz. The closed triangles correspond to the average values of the experimental measurements obtained from [63]. The gray line corresponds to the theoretical prediction made using the two-atom correlation signal $\eta(t)$ given by Eq. (14) [48], while the blue line represents the SEAQT prediction using the norm of the commutator operator $\|C\|$ as a direct indicator of how the coherence of the electromagnetic field mode is dissipated in time. Initially, the system should, if it were ideal, be maximally coherent with a magnitude of 0.5 for both the norm and two-atom correlation signal. However, it is not and thus the initial magnitude of the coherence has been moved (both for the correlation signal and the norm), in accord with [48,63], from a value of 0.5 to a value of 0.18 on the vertical axis to take into account experimental imperfections such as (i) the reflective quality of the mirrors in the cavity, which have a damping time (life of the photon inside the cavity) of 160 μs, (ii) noise in the detection of the atom, and (iii) inhomogeneities in the atomic beam caused by classical resonant microwave $\pi/2$ pulses applied at **R1** and **R2** [63,50]. In addition, the SEAQT prediction corresponds to a value of $\tau_A = \tau_F = 0.26\,T_R$ for the internal-relaxation times of the constituents in Eq. (2). This is very close to the characteristic decoherence time of $0.24\,T_R$ reported for the CQED experiment in [63]. As can be seen, the SEAQT model predicts the experimental data very well. A very slight deviation from the experimental values is observed with the fourth and fifth values, but this is well within the error bars for the experimental values indicated in the figure. Also, note that, though inconclusive, the experimental data averages suggest that the coherence is destroyed at all times, i.e., that the decoherence indicator is always non-negative, which is consistent with the SEAQT predictions. This holds for the second experiment as well [see Fig. 13(b)] even though the

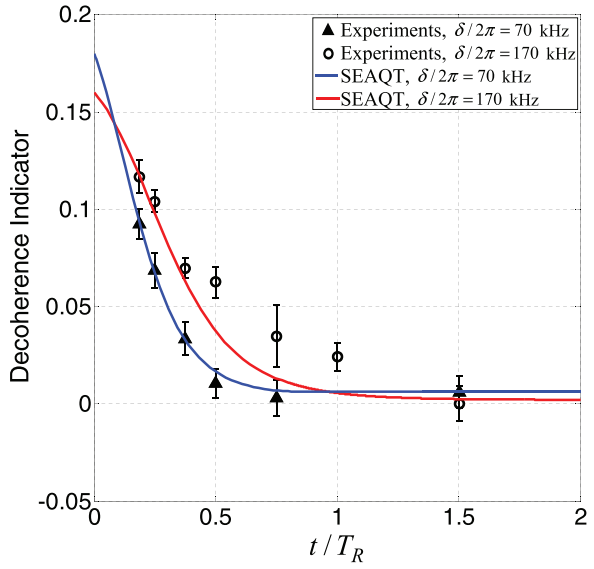

FIG. 14. (Color online) Comparison of the loss of coherence predicted by the SEAQT model with the CQED experimental results of Brune *et al.* [63].

uncertainties in the experimental data at $t/T_R = 1.5$ make this less of a certain conclusion.

Figure 13(b) depicts the comparison for a case with the detuning parameter $\delta/2\pi = 170$ kHz. The circles correspond to average values of the experimental measurements obtained from [63]. Again the gray line corresponds to the theoretical prediction made using the correlation signal $\eta(t)$ given by Eq. (14) [48]. The red line represents the SEAQT prediction using a value of $\tau_A = \tau_F = 0.36\,T_R$ for the internal-relaxation times of the constituents in the equation of motion. As for the case of Fig. 13(a), the maximum value of the theoretical predictions of $\eta(t)$ and the numerical predictions of SEAQT have been corrected to take into account experimental imperfections. The SEAQT model predicts the experimental data very well at the beginning and at the end of the decoherence evolution. A deviation from the experimental values is observed with the third, fourth, and fifth values, although it is also observed that the uncertainty associated with these measurements is higher than the rest of the experimental values reported.

Finally, Fig. 14 shows the SEAQT decoherence prediction of the experimental data of [63] in a single figure for the two values of the detuning parameter. Another interesting feature observed here is that, as seen in the experiments [63], the decoherence takes place at a faster rate for smaller values of detuning when the separation of the two state components of the photon field increase. This is captured with the SEAQT model. In addition, the coherence for the case of a detuning of $\delta/2\pi = 170$ kHz is smaller than for a detuning of $\delta/2\pi = 70$ kHz at the last experimental value of the evolution. This behavior is also captured by the SEAQT model.

VII. CONCLUSION

In this paper, an approach based on the principle of SEA was used in which a nonlinear model dynamics of the state evolution was embedded in the equation so as to describe in a thermodynamically consistent way the decoherence and decorrelation that occur during relaxation to equilibrium of the two simplest composite systems found in nature. The first composite system consists of two interacting correlated particles of type spin $\frac{1}{2}$ and the second consists of an atom interacting with a photon field.

For the two-spin-$\frac{1}{2}$-particle composite system, results show that the local coherence within each constituent (particle) disappears in a very short period of time, whereas the nonlocal coherence belonging to the composite system takes a very long time to disappear. In addition, the conjecture previously stated in [34] that the dissipation term of the SEAQT equation of motion is capable of only destroying correlations between constituents is heuristically confirmed by randomly creating and modeling the state evolution for 5000 randomly generated initial nonequilibrium states. The closest random initial nonequilibrium state to a pure state corresponds to a quantum purity of 0.86 and that closest to stable equilibrium corresponds to a quantum purity of 0.28. For the atom-photon field composite system, the decoherence phenomenon predicted with the SEAQT model was compared to the experimental data of Brune *et al.* [63] for two values of the detuning parameter, i.e., $\delta/2\pi = 70$ and 170 kHz. The comparison for both values shows that the SEAQT prediction is in good agreement with the experiments.

Finally, the results obtained demonstrate that the dynamic approach utilized in this paper is a robust and comprehensive framework for simulating the nonlinear dynamics encountered in complex quantum systems. As a predictive tool, the model has the potential to be useful in finding ways of controlling the decoherence, which is an impediment to the development of quantum computers, quantum communication devices, atomic clocks, etc. Applications to a whole variety of nonreactive and reactive quantum systems are possible and are already being developed.

ACKNOWLEDGMENTS

S.C.A. and M.R.v.S. would like to thank the National Council of Science and Technology (Mexico) for financial support through Assistantship No. 308141 (scholar ID 213158). G.P.B. gratefully acknowledges the Cariplo–UniBS-MIT-MechE faculty exchange program cosponsored by UniBS and the CARIPLO Foundation (Italy) under Grant No. 2008-2290.

[1] W. H. Zurek, Decoherence, einselection, and the quantum origins of the classical, Rev. Mod. Phys. **75**, 715 (2003).

[2] W. H. Zurek, Decoherence and the transition from quantum to classical-Revisited, Prog. Math. Phys. **48**, 1 (2007).

[3] M. A. Nielsen and I. L. Chuang, *Quantum Computation and Quantum Information* (Cambridge University Press, Cambridge, 2000).

[4] C. Bennett and D. P. DiVicenzo, Quantum information and computation, Nature (London) **404**, 247 (2000).

[5] A. Ardavan, O. Rival, J. J. L. Morton, S. J. Blundell, A. M. Tyryshkin, G. A. Timco, and R. E. P. Winpenny, Will spin-relaxation times in molecular magnets permit quantum information processing? Phys. Rev. Lett. **98**, 057201 (2007).

[6] D. S. Naik, C. G. Peterson, A. G. White, A. J. Berglund, and P. G. Kwiat, Entangled state quantum cryptography: Eavesdropping on the Ekert protocol, Phys. Rev. Lett. **84**, 4733 (2000).

[7] M. Baur, A. Fedorov, L. Steffen, S. Filipp, M. P. da Silva, and A. Wallraff, Benchmarking a quantum teleportation protocol in superconducting circuits using tomography and an entanglement witness, Phys. Rev. Lett. **108**, 040502 (2012).

[8] M. Nakatani and T. Ogawa, Quantum master equations for composite systems: Is Born-Markov approximation really valid? J. Phys. Soc. Jpn. **79**, 084401 (2010).

[9] X. Z. Yuan, H. S. Goan, and K. D. Zhu, Non-Markovian reduced dynamics and entanglement evolution of two coupled spins in a quantum spin environment, Phys. Rev. B **75**, 045331 (2007).

[10] G. Lindblad, On the generators of quantum dynamics semigroups, Commun. Math. Phys. **48**, 119 (1976).

[11] U. Weiss, *Quantum Dissipative Systems* (World Scientific, Singapore, 1999).

[12] K. Blum, *Density Matrix Theory and Applications*, 2nd ed. (Plenum, New York, 1996).

[13] M. R. von Spakovsky and J. Gemmer, Some trends in quantum thermodynamics, Entropy **16**, 3434 (2014).

[14] K. Kraus, General state changes in quantum theory, Ann. Phys. (NY) **64**, 311 (1971).

[15] V. Gorini, A. Kossakowski, and E. C. G. Sudarshan, Completely positive dynamical semigroups of N-level systems, J. Math. Phys. **17**, 821 (1976).

[16] H. P. Breuer and F. Petruccione, *Open Quantum Systems* (Oxford University Press, Oxford, 2002).

[17] J. Gemmer, M. Michel, and G. Mahler, *Quantum Thermodynamics* (Springer, Berlin, 2009).

[18] S. Goldstein, J. L. Lebowitz, R. Tumulka, and N. Zanghi, Long-time behavior of macroscopic quantum systems. Commentary accompanying the english translation of John von Neumann's 1929 article on the quantum ergodic theorem, Eur. Phys. J. H **35**, 173 (2010).

[19] E. Lubkin, Entropy of an *n*-system from its correlation with a *k*-reservoir, J. Math. Phys. **19**, 1028 (1978).

[20] S. Goldstein, J. Lebowitz, R. Tumulka, and N. Zanghì, Canonical typicality, Phys. Rev. Lett. **96**, 050403 (2006).

[21] P. Reimann, Typicality for generalized microcanonical ensembles, Phys. Rev. Lett. **99**, 160404 (2007).

[22] S. Popescu, A. J. Short, and A. Winter, Entanglement and the foundations of statistical mechanics, Nat. Phys. **2**, 754 (2006).

[23] Q. A. Turchete, C. J. Myatt, B. E. King, C. A. Sackett, D. Kielpinski, W. M. Itano, C. Monroe, and D. J. Wineland, Decoherence and decay of motional quantum states of a trapped atom coupled to engineered reservoirs, Phys. Rev. A **62**, 053807 (2000).

[24] D. F. Walls, Higher order effects in the master equation for coupled systems, Z. Phys. **234**, 231 (1970).

[25] H. J. Carmichael and D. F. Walls, Master equation for strongly interacting systems, J. Phys. A **6**, 1552 (1973).

[26] B. Misra, I. Prigogine, and M. Courbage, From deterministic dynamics to probabilistic descriptions, Physica A **98**, 1 (1979).

[27] B. Misra, I. Prigogine, and M. Courbage, Lyapounov variable: Entropy and measurement in quantum mechanics, Proc. Natl. Acad. Sci. USA **76**, 4768 (1979).

[28] I. Prigogine, What is entropy? Naturwissenschaften **76**, 1 (1989).

[29] I. E. Antoniou and I. Prigogine, Intrinsic irreversibility and integrability of dynamics, Physica A **192**, 443 (1993).

[30] J. L. Park, Nature of quantum states, Am. J. Phys. **36**, 211 (1968).

[31] G. N. Hatsopoulos and E. P. Gyftopoulos, A unified quantum theory of mechanics and thermodynamics. Part I. Postulates, Found. Phys. **6**, 15 (1976).

[32] R. F. Simmons and J. L. Park, The essential nonlinearity of N-level quantum thermodynamics, Found. Phys. **11**, 297 (1981).

[33] G. P. Beretta, E. P. Gyftopoulos, J. L. Park, and G. N. Hatsopoulos, Quantum thermodynamics. A new equation of motion for a single constituent of matter, Nuovo Cimento B **82**, 169 (1984).

[34] G. P. Beretta, E. P. Gyftopoulos, and J. L. Park, Quantum thermodynamics. A new equation of motion for a general quantum system, Nuovo Cimento B **87**, 77 (1985).

[35] G. N. Hatsopoulos and G. P. Beretta, Where is the entropy challenge? in *Meeting the Entropy Challenge: An International Thermodynamics Symposium in Honor and Memory of Professor J. H. Keenan*, edited by G. P. Beretta, A. F. Ghoniem, and G. N. Hatsopoulos, AIP Conf. Proc. Ser. 1033 (AIP, New York, 2008), pp. 34–54.

[36] R. F. Simmons and J. L. Park, On completely positive maps in generalized quantum dynamics, Found. Phys. **11**, 47 (1981).

[37] S. Gheorghiu-Svirschevski, Nonlinear quantum evolution with maximal entropy production, Phys. Rev. A **63**, 022105 (2001).

[38] S. Gheorghiu-Svirschevski, Addendum to "Nonlinear quantum evolution with maximal entropy production," Phys. Rev. A **63**, 054102 (2001).

[39] A. Bohm, S. Maxson, and M. Loewe, Microphysical irreversibility in quantum mechanics, Rep. Math. Phys. **36**, 245 (1995).

[40] A. Bohm, S. Maxson, M. Loewe, and M. Gadella, Quantum mechanical irreversibility, Physica A **236**, 485 (1997).

[41] D. Schuch and K. M. Chung, From macroscopic irreversibility to microscopic reversibility via a nonlinear Schrödinger-type field equation, Int. J. Quantum Chem. **29**, 1561 (1986).

[42] G. P. Beretta, in *The Physics of Phase Space (Nonlinear Dynamics and Chaos Geometric Quantization, and Wigner Function)*, edited by Y. S. Kim and W. W. Zachary, Lecture Notes in Physics Vol. 278 (Springer, Berlin, 1986), pp. 441–443.

[43] G. P. Beretta, Maximum entropy production rate in quantum thermodynamics, J. Phys. Conf. Ser. **237**, 012004 (2010).

[44] G. P. Beretta, Steepest entropy ascent model for far-nonequilibrium thermodynamics: Unified implementation of the maximum entropy production principle, Phys. Rev. E **90**, 042113 (2014).

[45] C. E. Smith and M. R. von Spakovsky, Comparison of the non-equilibrium predictions of quantum thermodynamics at the atomistic level with experimental evidence, J. Phys. Conf. Ser. **380**, 012015 (2012).

[46] X. Zhou, I. Dotsenko, B. Peaudecerf, T. Rybarczyk, C. Sayrin, S. Gleyzes, J. M. Raimond, M. Brune, and S. Haroche, Field locked to a Fock state by quantum feedback with single photon corrections, Phys. Rev. Lett. **108**, 243602 (2012).

[47] S. Haroche, M. Brune, and J. M. Raimond, Atomic clocks for controlling light fields, Phys. Today **66**(1), 27 (2013).

[48] J. M. Raimond, M. Brune, and S. Haroche, Reversible decoherence of a mesoscopic superposition of field states, Phys. Rev. Lett. **79**, 1964 (1997).

[49] S. Deleglise, I. Dotsenko, C. Sayrin, J. Bernu, M. Brune, J. M. Raimond *et al.*, Reconstruction of non-classical cavity field states with snapshots of their decoherence, Nature (London) **455**, 510 (2008).

[50] S. Haroche and J. M. Raimond, *Exploring the Quantum* (Oxford University Press, Oxford, 2006).

[51] J. M. Raimond and S. Haroche, in *Quantum Decoherence*, edited by B. Duplantier, J. M. Raimond, and V. Rivasseau, Progress in Mathematical Physics Series (Birkhäuser, Basel, 2007), Vol. 48, pp. 33–83.

[52] M. Brune, F. Schmidt-Kaler, A. Maali, J. Dreyer, E. Hagley, J. M. Raimond, and S. Haroche, Quantum Rabi oscillation: A direct test of field quantization in a cavity, Phys. Rev. Lett. **76**, 1800 (1996).

[53] J. M. Raimond, M. Brune, and S. Haroche, Manipulating quantum entanglement with atoms and photons in a cavity, Rev. Mod. Phys. **73**, 565 (2001).

[54] Q. A. Turchette, D. Kielpinski, B. E. King, D. Leibfried, D. M. Meekhof, C. J. Myatt, M. A. Rowe, C. A. Sackett, C. S. Wood, W. M. Itano, C. Monroe, and D. J. Wineland, Heating of trapped ions from the quantum ground state, Phys. Rev. A **61**, 063418 (2000).

[55] A. Montefusco, F. Consonni, and G. P. Beretta, Essential equivalence of the GENERIC and Steepest Entropy Ascent models of dissipation for non-equilibrium thermodynamics, arXiv:1411.5378 (2014).

[56] J. Maddox, Uniting mechanics and statistics, Nature (London) **316**, 11 (1985).

[57] M. Ferrero, D. Salgado, and J. L. Sánchez-Gómez, Nonlinear quantum evolution does not imply supraluminal communication, Phys. Rev. A **70**, 014101 (2004).

[58] A. Peres, Nonlinear variants of Schrödinger's equation violate the second law of thermodynamics, Phys. Rev. Lett. **63**, 1114 (1989).

[59] G. P. Beretta, Nonlinear model dynamics for closed-system, constrained, maximal-entropy-generation relaxation by energy redistribution, Phys. Rev. E **73**, 026113 (2006).

[60] G. P. Beretta, A theorem on Lyapunov stability for dynamical systems and a conjecture on a property of entropy, J. Math. Phys. **27**, 305 (1986).

[61] G. P. Beretta, On the general equation of motion of quantum thermodynamics and the distinction between quantal and non-quantal uncertainties, Ph.D. thesis, Massachusetts Institute of Technology, 1981, arXiv:quant-ph/0509116.

[62] G. P. Beretta, Nonlinear quantum evolution equations to model irreversible adiabatic relaxation with maximal entropy production and other nonunitary processes, Rep. Math. Phys. **64**, 139 (2009).

[63] M. Brune, E. Hagley, J. Dreyer, X. Maitre, A. Maali, C. Wunderlich, J. M. Raimond, and S. Haroche, Observing the progressive decoherence of the "meter" in a quantum measurement, Phys. Rev. Lett. **77**, 4887 (1996).

[64] G. P. Beretta, Nonlinear extensions of Schrödinger–von Neumann quantum dynamics: A set of necessary conditions for compatibility with thermodynamics, Mod. Phys. Lett. A **20**, 977 (2005).

[65] J. Gemmer and G. Mahler, Entanglement and the factorization-approximation, Eur. Phys. J. D **17**, 385 (2001).

[66] W. K. Wootters, Statistical distance and Hilbert space, Phys. Rev. D **23**, 357 (1981).

[67] P. Salamon, J. D. Nulton, and R. S. Berry, Length in statistical thermodynamics, J. Chem. Phys. **82**, 2433 (1985).

[68] S. L. Braunstein and C. M. Caves, Statistical distance and the geometry of quantum states, Phys. Rev. Lett. **72**, 3439 (1994).

[69] E. P. Gyftopoulos and E. Çubukçu, Entropy: Thermodynamic definition and quantum expression, Phys. Rev. E **55**, 3851 (1997).

[70] E. P. Gyftopoulos and G. P. Beretta, in *Thermodynamics: Foundations and Applications* (Dover, Mineola, 2005), p. 62.

[71] E. Weisstein, Sphere Point Picking, 2013, Wolfram MathWorld, available at http://mathworld.wolfram.com/SpherePointPicking.html

[72] J. M. Fink, M. Göppl, M. Baur, R. Bianchetti, P. J. Leek, A. Blais, and A. Wallraff, Climbing the Jaynes-Cummings ladder and observing its nonlinearity in a cavity QED system, Nature (London) **454**, 315 (2008).

[73] K. Fujii and T. Suzuki, An approximate solution of the Jaynes–Cummings model with dissipation II: Another approach, Int. J. Geom. Methods Mod. Phys. **09**, 1250036 (2012).

[74] M. A. Marchiolli, Quantitative aspects of entanglement in the driven Jaynes-Cummings model, J. Mod. Opt. **53**, 2733 (2006).

[75] E. T. Jaynes and F. W. Cummings, Comparison of quantum and semiclassical radiation theories with application to the beam maser, Proc. IEEE **51**, 89 (1963).

[76] F. W. Cummings, Stimulated emission of radiation in a single mode, Phys. Rev. **140**, A1051 (1965).

[77] E. T. Jaynes, Some aspects of maser theory, Stanford University Microwave Laboratory Report No. 502, 1958 (unpublished).